Available online at www.sciencedirect.com
ScienceDirect
International Journal of Solids and Structures 43 (2006) 6948–6964
INTERNATIONAL JOURNAL OF SOLIDS and STRUCTURES
www.elsevier.com/locate/ijsolstr

Optimum design of shell structures with random geometric, material and thickness imperfections

Nikos D. Lagaros *, Vissarion Papadopoulos

Institute of Structural Analysis and Seismic Research, National Technical University of Athens, Athens 15780, Greece

Received 11 July 2005; received in revised form 20 December 2005
Available online 3 March 2006

Communicated by David A. Hills

Abstract

The optimum design of isotropic shell structures with random initial geometric, material and thickness imperfections is investigated in this paper and a robust and efficient methodology is presented for treating such problems. For this purpose, the concept of an initial "imperfect" structure is introduced involving not only geometric deviations of the shell structure from its perfect geometry but also a spatial variability of the modulus of elasticity as well as of the thickness of the shell. An efficient reliability-based design optimization (RBDO) formulation is proposed. The objective function is considered to be the weight of the structure while both deterministic and probabilistic constraints are taken into account. The overall probability of failure is taken as the global probabilistic constraint for the optimization procedure. Numerical results are presented for a cylindrical panel, demonstrating the efficiency as well as the applicability of the proposed methodology in obtaining rational optimum designs of imperfect shell-type structures.

Keywords: Evolutionary computations; Reliability-based design optimization; Nonlinear shell finite element; Random imperfections; Spectral representation

1. Introduction

A typical engineering task during the development of any structural system is, among others, to improve its performance in terms of constructional cost and structural response. Improvements can be achieved either by simply using design criteria based on existing codes and experience or on an automated way by using optimization methods that lead to a structural design which can be considered as the optimum one. Strictly speaking, optimal design means that no better solution exists under certain constraints. In practical applications however, finding the global optimum solution is a very difficult task, due to the uncertainty or scatter involved in various structural parameters such as material properties, geometric imperfections, loading variations,

* Corresponding author. Tel.: +30 1 7722625; fax: +30 1 7721693.
E-mail addresses: nlagaros@central.ntua.gr (N.D. Lagaros), vpapado@central.ntua.gr (V. Papadopoulos).

0020-7683/$ - see front matter © 2006 Elsevier Ltd. All rights reserved.
doi:10.1016/j.ijsolstr.2006.02.019

uncertain boundary conditions, etc. For this reason it is generally recognized that a deterministic based formulation of a structural optimization problem, which ignores the uncertainty involved in the various aforementioned parameters, can not reach to an unbiased, feasible and realistic optimum design. Once a deterministic optimum solution is implemented in a real physical system, its optimal performance may vanish because of the parameters' scatter, which is unavoidable and might also be unfavorable since the performance of the ''implemented'' design may be far worse than the one expected.

In order to account for the randomness of the various structural parameters affecting the structural response, probabilistic formulations of the optimization problem have been developed over the last decades (Schueller, 2001; Hurtado and Barbat, 1997). Most of the aforementioned formulations are based on reliability analysis methodologies and have stimulated the interest for the probabilistic optimum design of structures. There are two distinguished design formulations that account for the probabilistic systems response: robust design optimization (RDO) (Lagaros et al., 2005; Lee and Park, 2001; Messac and Ismail-Yahaya, 2002) and reliability-based design optimization (RBDO) (Papadrakakis and Lagaros, 2002; Qu et al., 2003; Allen and Maute, 2005). RDO methods primarily seek to minimize the influence of stochastic variations on the mean and variance of critical response variables, such as critical displacements and/or stresses. On the other hand, the main goal of RBDO methods is to design for safety with respect to extreme events. In a RBDO formulation, probabilistic constraints are incorporated into the optimization procedure leading to unbiased estimates of the structural performance and subsequently, to the determination of design points that are located within a range of target failure probabilities.

During the last fifteen years there has been a growing interest on optimization algorithms that rely on analogies to natural processes such as evolutionary algorithms (EA). For complex and realistic structural optimization problems, EA methods appear to be the only reliable approach, since most mathematical programming optimizers are prone to converge to a local optimum or may not converge at all (Papadrakakis et al., 1999; Lagaros et al., 2002). Based on previous experience regarding the relative superiority of evolution strategies (ES) over the mathematical programming (MP) methods and some of the EA methods in some problems (Papadrakakis et al., 1999; Lagaros et al., 2002), the ES optimization algorithm was selected for the solution of the optimization problem at hand.

In the present study a RBDO formulation using EA is implemented in a reliability-based sizing-shape optimization of shell-type structures with random initial geometric material and thickness imperfections. It is well-known that the response behavior of shell structures is generally influenced by their initial imperfections, which occur during the manufacturing and construction stages. In addition, variability of initial imperfections together with their pronounced influence on the load carrying capacity of shells has been proved to be responsible for the large scatter observed in the experimental results (Deml and Wunderlich, 1997; Schenk and Schueller, 2003; Li et al., 1997; Palassopoulos, 1997). Also other sources of imperfections such as the variability of thickness, material properties, boundary conditions and misalignment of loading are also responsible for the reduction as well as the scatter of the buckling load of shell structures (Schenk and Schueller, 2003; Li et al., 1997; Papadopoulos and Papadrakakis, 2004, 2005). In the majority of studies, these influencing parameters have not been treated as stochastic variables in a rational manner. Therefore, an accurate prediction of the structural performance of shell-type structures requires a realistic modeling of all uncertainties involved in conjunction with a robust finite element formulation that can efficiently and accurately handle the geometric as well as physical nonlinearities of shell type structures (Li et al., 1997; Papadopoulos and Papadrakakis, 2005).

In particular the effect of material and thickness imperfections on the buckling load of isotropic shells is investigated with respect to the optimum design of a cylindrical panel. For this purpose, the concept of an initial ''imperfect'' structure is introduced involving not only geometric deviations of the shell structure from its perfect geometry but also a spatial variability of the modulus of elasticity as well as of the thickness of the shell. These combined ''imperfections'' are incorporated in an efficient and cost effective nonlinear stochastic finite element formulation of the TRIC shell element (Argyris et al., 1997, 1998, 2002a; Argyris et al., 2002b) using the local average method for the derivation of the stochastic stiffness matrix, while the variability of the limit loads is obtained by means of a brute-force Monte Carlo simulation (MCS) procedure. All types of imperfections are modeled as two-dimensional univariate homogeneous stochastic fields (2D-1V) using the spectral representation method (Shinozuka and Deodatis, 1996).

For the RDBO formulation, the objective function is assumed to be the weight of the structure while the constraints are taken both deterministic (stress limitations) and probabilistic (the overall probability of failure of the structure). The probabilistic constraint enforces the condition that the probability failure, of the system is smaller than a certain value. It is assumed that structural failure occurs when buckling load of the shell is reached. Then, the overall probability of failure is taken as the global probabilistic constraint. The numerical results demonstrate the efficiency as well as the applicability of the proposed methodology in obtaining rational optimum designs of shell-type structures in the presence of random geometric, material and thickness imperfections.

2. Reliability-based structural optimization

In the present study, the reliability-based sizing-shape optimization of a cylindrical panel with random geometric material and thickness imperfections is investigated. In the deterministic structural optimization problems, the aim is to minimize the weight of the structure under certain deterministic behavioral constraints usually on stresses and displacements. In reliability-based structural optimal design, additional probabilistic constraints are imposed in order to take into account various random parameters and to ensure that the probability of failure of the structure is within acceptable limits. The probabilistic constraints enforce the condition that the probability failure of the system is smaller than a certain value (i.e., 10^{-3}). In this work the overall probability of failure of the structure is taken as the global probabilistic constraint.

Through the constraints considered in the formulation of the optimization problem, it is ensured that the performance of the shell meets the design requirements. The von Mises yield criterion is employed in order to assess the value of an equivalent stress that will be compared with the yield stress σ_y. Therefore, the following expression has to be satisfied for each triangular shell element:

$$\sqrt{\sigma_1^2+\sigma_2^2-3\sigma_1\sigma_2+3\tau^2}\leqslant \sigma_y/\gamma_{M0}, \tag{1}$$

where σ_1, σ_2, τ are the stresses in the middle surface of the triangle and γ_{M0} is a safety factor equal to 1.10, according to Eurocode 3 (1993).

An RBDO problem can be formulated in the following form

$$\begin{aligned} &\text{min} && F(s)\\ &\text{subject to} && g_j(s)\leqslant 0, \quad j=1,\ldots,m,\\ &&& \Pr(h_i(s,x)\leqslant 0)\leqslant p_{a,i}, \quad i=1,\ldots,n,\\ &\text{where} && s\in R^{n_s},\\ &&& x\sim N(\mu_x,\sigma_x^2), \end{aligned} \tag{2}$$

$F(s)$ is the objective function (i.e., the structural weight), s is the vector of geometric design variables, x is the vector of random variables, $g_j(s)$ are the deterministic constraints and $h_i(s,x)$ are the constraints that their probability of violation should be less than an allowable probability $p_{a,i}$. In this work the overall probability of failure of the structure is considered as the probabilistic constraint.

The proposed reliability-based sizing-shape optimization methodology proceeds with the following steps:

1. At the outset of the optimization procedure the geometry, the boundaries and the reference loads of the structure under investigation are defined.
2. The optimization problem of Eq. (2) is defined selecting the constraint functions, deterministic and probabilistic ones.
3. The optimization phase is carried out with evolution strategies where feasible designs are produced at each optimization cycle. The feasibility of the designs is checked for each design vector with respect to both deterministic and probabilistic constraints considered.
4. The satisfaction of the deterministic constraints is monitored through a linear finite element analysis of the structure using the linear TRIC shell element.

5. The satisfaction of the probability constraints is monitored via a reliability analysis of the "imperfect" structure. The probability of failure for each set of design variables is calculated using a brute-force MCS in conjunction with a geometric and material nonlinear analysis in order to compute the corresponding buckling loads of the shell.
6. If the convergence criteria for the optimization algorithm are satisfied then the optimum solution has been found and the process is terminated, else the whole process is repeated.

3. Finite element formulation

The finite element simulation is performed with the triangular element TRIC, which is based on the natural mode method. The TRIC shear-deformable facet shell element is a reliable and cost-effective element suitable for linear and nonlinear analysis of thin and moderately thick isotropic as well as composite plate and shell structures. For the sake of completeness, a brief description of the TRIC shell element is given in this section. Extensive reports on the formulation of TRIC may be found in Argyris et al. (1997, 1998, 2002a).

The TRIC element has 18 degrees of freedom (6 per node) and hence 12 natural straining modes (Fig. 1). Three natural axial strains and natural transverse shear strains are measured parallel to the edges of the triangle. The stiffness is contributed by deformations only and not by the associated rigid body motions. The natural stiffness matrix can be produced from the statement of variation of the strain energy with respect to the natural coordinates.

The geometric stiffness is based on large deflections but small strains and consists of two parts. A simplified geometric stiffness matrix generated by the rigid-body movements of the element and the natural geometric stiffness matrix due to the coupling between the axial forces and the symmetric bending modes (stiffening or softening effect). To construct the geometric stiffness we consider small rigid-body rotational increments about the local Cartesian axes. These rigid-body rotational increments correspond to nodal Cartesian moments along the same axes. Using the fact that the resultants of all forces produced by rigid-body motion must vanish, we arrive at the expression for the local rigid-body rotational simplified geometric stiffness. The term simplified refers to the fact that only the middle plane axial natural forces are included in the stiffness matrix, which fully represents the prestress state within the material. Once the simplified geometric stiffness is formed it may transformed to the global coordinate system. In addition to the geometric stiffness corresponding to the rigid-body movements of the element, an approximate natural geometric stiffness arising from

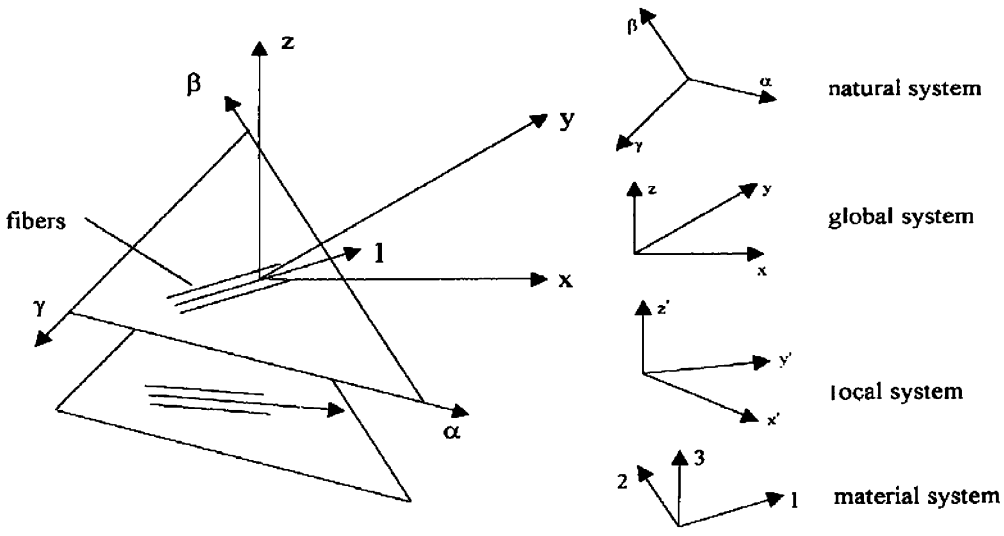

Fig. 1. The multilayer triangular TRIC element; coordinate systems.

the coupling between the axial forces and the symmetric bending mode (stiffening or softening effect) is also considered.

The elastoplastic constitutive matrix is established by obtaining the relation between the natural strain and stress increments for each layer r within a given load step:

$$\mathrm{d}\sigma_c^r = \left[\kappa_{ct}^{\mathrm{el}} - \frac{1}{H + s_{\mathrm{N}}^{\mathrm{t}}\kappa_{ct}^{\mathrm{el}}s_{\mathrm{N}}}(\kappa_{ct}^{\mathrm{el}}s_{\mathrm{N}})(\kappa_{ct}^{\mathrm{el}}s_{\mathrm{N}})^{\mathrm{t}}\right]^r \mathrm{d}\gamma_t^r, \tag{3}$$

where H is the hardening parameter and S_{N} is obtained by the normality flow rule as

$$s_{\mathrm{N}} = \frac{\partial F}{\partial \sigma_c} = \left[\frac{\partial F}{\partial \sigma_{c\alpha}}\frac{\partial F}{\partial \sigma_{c\beta}}\frac{\partial F}{\partial \sigma_{c\gamma}}\right]^{\mathrm{t}}, \tag{4}$$

and the expression in brackets corresponds to the elastoplastic material stiffness matrix $\kappa_{ct}^{\mathrm{el-pl}}$ valid for every layer r.

$$[\kappa_{ct}^{\mathrm{el-pl}}]^r = \left[\kappa_{ct}^{\mathrm{el}} - \frac{1}{H + s_{\mathrm{N}}^{\mathrm{t}}\kappa_{ct}^{\mathrm{el}}s_{\mathrm{N}}}(\kappa_{ct}^{\mathrm{el}}s_{\mathrm{N}})(\kappa_{ct}^{\mathrm{el}}s_{\mathrm{N}})^{\mathrm{t}}\right]^r. \tag{5}$$

The natural elastoplastic stiffness of the element is obtained by summing up the natural elastoplastic layer stiffnesses of the element. A full description of the linear elastic, geometric and elastoplastic stiffness matrix of the TRIC shell element can be found in Argyris et al. (1997, 1998, 2002a), respectively.

4. Stochastic description of initial imperfect geometry

The problem of buckling of shells has received a great deal of interest in the last decades. The major problem has always been the great discrepancy between theoretically expected and experimentally observed buckling loads and also the wide scatter in those measured limit loads. It was soon realized, that the buckling behavior of shells is generally influenced by their initial geometric imperfections, which produced through the manufacturing procedure. Additional researches showed that the initial geometric imperfections is not the only reason of the discrepancy and the scatter, and that the effect of thickness variability, material imperfections and imperfect boundary conditions proved to be of great importance, too. Since the use of powerful computers became easier than ever, the analysis of such structures has been carried out through applications of the finite element method in conjunction with a stochastic description of the uncertainties involved in all kinds of previously mentioned imperfections (Deml and Wunderlich, 1997; Li et al., 1997; Palassopoulos, 1997; Arbocz, 2001; Elishakoff, 2000; Elishakoff and Arbocz, 1982, 1985; Elishakoff et al., 1987; Arbocz and Hol, 1991).

For the above mentioned stochastic finite element modeling, the imperfect geometry of shell-type structures is usually represented as a two-dimensional univariate stochastic field. The statistical properties of this underlying field modeling the initial geometric imperfections can be based either on experimental measurements, or on assumed in cases where no experimental results are available. Previous work on the subject (Schenk and Schueller, 2003; Papadopoulos and Papadrakakis, 2004) has focused mainly on the buckling behavior of axially compressed cylinders for which a data bank of experimentally measured initial imperfections is available (Arbocz and Abramovich, 1979). In this early work, the stochastic description of the geometric imperfections was based on a statistical analysis of the experimentally measured imperfections. The results obtained clearly demonstrated that the stochastic field of the initial geometric imperfections is non-homogeneous, while the Gaussian distribution fits well the experimental data.

In the present paper initial geometric imperfections are modeled as a homogeneous two-dimensional Gaussian stochastic field. While the Gaussian assumption for the probability density function fits well the aforementioned experimental data, the assumption of homogeneity is not generally applicable for the description of initial imperfections of shells. However this assumption is adopted in this study and elsewhere (Schenk and Schueller, 2003; Papadopoulos and Papadrakakis, 2004, 2005), for simplicity and due to the fact that there are no experimental data available for this particular type of cylindrical panels. For this reason, a parametric study was performed in previous investigations by Papadopoulos and Papadrakakis (2004, 2005), with respect to the correlation lengths of the stochastic fields in both x and y directions. The outcome of the parametric

study was the evaluation of the "worst" imperfection mode of the shell. As explained in detail in the Numerical examples section, this "worst" imperfections' pattern was adopted subsequently in the optimization procedure.

For the description of the initial geometric imperfections, the radius of the structure is assumed to be a 2D-1V homogeneous stochastic field with respect to the perfect geometry

$$r(x,y) = r_0 + f_1(x,y) \times h, \tag{6}$$

where r_0 is the radius of the perfect geometry, $f_1(x,y)$ is a zero mean Gaussian homogeneous stochastic field and h is the height of the cylindrical panel. In the present paper the amplitude of the imperfections, which is controlled by the standard deviation of the stochastic field, is selected to be a percentage of the height h of the cylindrical panel. The coordinates x and y are the global Cartesian coordinates of the unfolded panel.

Moreover, the shape of the imperfections is controlled by the correlation lengths of the stochastic field $f_1(x,y)$ in directions x and y, respectively. As mentioned previously, these correlation lengths are usually derived from experimental data and play a significant role on the buckling behavior of shells (Schenk and Schueller, 2003; Papadopoulos and Papadrakakis, 2005). Since no experimental data are available for this type of problems, a parametric study was performed in Papadopoulos and Papadrakakis (2004, 2005), with respect to the correlation lengths of the stochastic field in both x and y directions. The outcome of this parametric study was the evaluation of the "worst" imperfection mode of the shell which leads to the estimation of the lower bound of the buckling load of the shell. This information is most valuable for the safe design of shells against buckling (Deml and Wunderlich, 1997; Palassopoulos, 1997).

5. Stochastic stiffness matrix

The modulus of elasticity as well as the thickness of the structure are also considered in the present study as "imperfections", due to their spatial variability. Therefore, these parameters are also described by two independent 2D-1V homogeneous stochastic fields

$$E(x,y) = E_0[1 + f_2(x,y)], \tag{7}$$

$$t(x,y) = t_0[1 + f_3(x,y)], \tag{8}$$

where E_0 is the mean value of the elastic modulus, t_0 is the mean thickness of the structure and $f_2(x,y)$, $f_3(x,y)$ are two zero mean Gaussian homogeneous stochastic fields corresponding to the variability of the modulus of elasticity and the thickness of the shell, respectively. In the present study, stochastic fields $f_2(x,y)$ and $f_3(x,y)$ are assumed uncorrelated. However, since cross-correlation between the aforementioned fields has proven to play an important role on the buckling behavior of shell-type structures leading often to a further reduction of the bearing capacity, with respect to the uncorrelated case (Noh and Kwak, 2006; Noh, 2006; Stefanou and Papadrakakis, 2004), the effect of the above mentioned correlation in the optimum design of shell structures will be specifically addressed in follow-up research.

The stochastic stiffness matrix of the shell element is derived using the local average method. This method has been used extensively by many researchers in conjunction with the stochastic finite element method (SFEM). In a recent study by Argyris et al. (2002b), it was shown that for shell type structures, the local average method is not only superior to the weighted integral method in terms of simplicity and computational efficiency and the accuracy of the results are very close to those of the weighted integral method. Given a stochastic field $f(x,y,z)$, the local average method provides discretized values of the field as follows:

$$f_i = \frac{1}{V_i} \int_{V_i} f(x,y,z)\, \mathrm{d}V_i, \tag{9}$$

where V_i is the domain over which the integration has to be performed. In the case of stochastic finite elements, the domain represents the length (truss and beam elements), the area (plain stress/strain, plate, shell elements) or the volume (3D solid elements) of the ith element. It is obvious that, according to this method, a single random variable per finite element is used to delineate the stochastic field since its random characteristics are represented by the local spatial average over each element. In this context the stochastic element stiffness matrix is expressed as

$$k^{(e)} = \left(1 + \alpha^{(e)}\right) k_0^{(e)}, \tag{10}$$

where

$$\alpha^{(e)} = \frac{1}{V^{(e)}} \int_{V^{(e)}} f^{(e)}(x, y, z)\, \mathrm{d}V^{(e)}. \tag{11}$$

In the case where both the modulus of elasticity and the thickness are assumed to be simultaneously stochastic, the random variable $\alpha^{(e)}$ is given by

$$\alpha^{(e)} = \alpha_1^{(e)} \alpha_2^{(e)}, \tag{12}$$

where $\alpha_1^{(e)}$ and $\alpha_2^{(e)}$ are the local averages corresponding to the stochastic fields of the modulus of elasticity and thickness, respectively.

6. Monte Carlo simulation

The generation of sample functions for stochastic fields $f_1(x, y)$, $f_2(x, y)$ and $f_3(x, y)$ corresponding to the variations of the geometric, material and thickness imperfections, respectively, is performed using the spectral representation method (Shinozuka and Deodatis, 1996). The simulation points of the stochastic fields are located at the center of gravity of the TRIC shell elements. Therefore, the stochastic fields are simulated in non-uniformly spaced points of the structure. For this reason, the series of cosines formula is chosen for the simulation of the stochastic fields instead of the fast Fourier transform (FFT) which requires that the stochastic field is simulated at uniformly spaced points. The two-sided power spectral density function used for the description of the above mentioned fields is assumed to correspond to an autocorrelation function of exponential type and is given by

$$S_{f_0 f_0}(\kappa_1, \kappa_2) = \frac{\sigma_f^2}{4\pi} b_1 b_2 \exp\left[-\frac{1}{4}\left(b_1^2 \kappa_1^2 + b_2^2 \kappa_2^2\right)\right], \tag{13}$$

where σ_f denotes the standard deviation of the stochastic field and, b_1 and b_2 denote the parameters that influence the shape of the spectrum which are proportional to the correlation distances of the stochastic field along the x_1 and x_2 axes, respectively. A large number N_{SAMP} of sample functions are produced, leading to the generation of a set of stochastic stiffness matrices. For the reliability analysis required at each step of the optimization procedure, the associated structural problem is solved N_{SAMP} times, while the probability of failure is finally be calculated in terms of sample mean as follows:

$$p_f = \frac{1}{N_\infty} \sum_{j=1}^{N_\infty} I(x_j) \tag{14}$$

in which $I(x_j)$ is an indicator for successful and unsuccessful simulations defined as

$$I(x_j) = \begin{cases} 1 & \text{if } G(x_j) \geqslant 0, \\ 0 & \text{if } G(x_j) < 0. \end{cases} \tag{15}$$

7. Evolutionary algorithms

The two most widely used optimization algorithms belonging to the class of evolutionary algorithms (EA) that imitate nature by using biological methodologies are the genetic algorithms (GA) and evolution strategies. In this work the ES method is used as the optimization tool for addressing the RBO problem, based on previous experience regarding the relative superiority of ES over the MP and GA methods in some specific problems (Papadrakakis et al., 1999; Lagaros et al., 2002). ES imitate biological evolution in nature and have three characteristics that make them differ from the gradient based optimization algorithms: (i) in place of the usual deterministic operators, they use randomized operators: recombination, mutation, selection; (ii) instead of a single design point, they work simultaneously with a population of design points; (iii) they can handle

continuous, discrete and mixed optimization problems (Schwefel, 1981). In the ES algorithm, each individual is equipped with a set of parameters

$$\begin{aligned} &a = [s, \sigma, \alpha] \in I_c, \\ &I_c = R^{n_s} \times R_+^{n_\sigma} \times [-\pi, \pi]^{n_a} \end{aligned} \tag{16}$$

where s is the vector of the design variables while vectors σ and α are the distribution parameter vectors. Vector $\sigma \in R_+^{n_\sigma}$ corresponds to the standard deviations ($1 \leqslant n_\sigma \leqslant n_s$) of the normal distribution while vector $\alpha \in [-\pi, \pi]^{n_a}$ corresponds to the inclination angles ($n_\alpha = (n_c - n_\sigma/2)(n_\sigma - 1)$), defining linearly correlated mutations of the continuous design variables s. Let $P_{\mathrm{p}}^{(t)} = \{a_1, \ldots, a_\mu\}$ denotes a parent population of individuals at the tth generation. The genetic operators used in the ES method are denoted by the following mappings:

$$\begin{aligned} &\mathrm{rec} : (I_c)^\mu \to (I_c)^\lambda \quad \text{recombination}, \\ &\mathrm{mut} : (I_c)^\lambda \to (I_c)^\lambda \quad \text{mutation}, \\ &\mathrm{sel}_\mu^k : (I_c)^k \to (I_c)^\mu \quad \text{selection}, \ k \in \{\lambda, \mu + \lambda\}. \end{aligned} \tag{17}$$

A single iteration of the ES, which is a step from the parent population $P_{\mathrm{p}}^{(t)}$ to the next generation parent population $P_{\mathrm{p}}^{(t+1)}$ is modeled by the mapping

$$\mathrm{opt}_{\mathrm{EA}} : (I_c)^\mu \to (I_c)^\mu. \tag{18}$$

7.1. Recombination

In any generation the μ-membered parent population $P_{\mathrm{p}}^{(t)}$ produce an λ-membered offspring population $P_{\mathrm{o}}^{(t)}$. For every offspring vector a temporary parent vector is first built by means of recombination. In our implementation the following recombination scheme has been used, $\mathrm{rec}_h : R^{n_h} \to R^{n_h}$ recombines the values of the vector h, where h corresponds to either a design variable vector or a distribution parameter vector

$$\mathrm{rec}_h(h) := (h_{a,1} \text{ or } h_{b,1}, \ldots, h_{a,n_b} \text{ or } h_{b,n_b}), \tag{19}$$

$h_{a,i}$ and $h_{b,i}$ are the ith components of the vector h_a and h_b which are two parent vectors randomly chosen from the population.

7.2. Mutation

The parameters σ and α determine the variances and covariances of the n_s-dimensional normal distribution, which is used for exploring the continuous part of the design space. The amount of parameters attached to an individual can vary, depending on the degree of freedom required by the objective function in question. The setting that is used in the current study is: $n_\sigma = n_s$, $n_\alpha = n_s(n_s - 1)/2$, which corresponds to the correlated mutation operator with a complete covariance matrix for each individual.

According to the generalized structure of the individuals of the populations in the proposed mixed-discrete EA algorithm, the mutation operator $\mathrm{mut} : I_c \to I_c$ is defined as follows:

$$\mathrm{mut} = [\mathrm{mu}_s \circ (\mathrm{mu}_\sigma \times \mathrm{mu}_\alpha)]. \tag{20}$$

The mutation operator is applied after the recombination operator to the intermediate individuals. The distribution parameters of the structure of an individual are mutated first. Mutation operator $\mathrm{mu}_\sigma : R_+^{n_\sigma} \to R_+^{n_\sigma}$ mutates the recombined values of the vector of standard deviation σ:

$$\mathrm{mu}_\sigma(\sigma) := (\sigma_1 \exp(z_1 + z_0), \ldots, \sigma_{n_\sigma} \exp(z_{n_\sigma} + z_0)), \tag{21}$$

where $z_0 \approx N(0, \tau_0^2)$, $z_i \approx N(0, \tau^2)$ $\forall i \in \{1, 2, \ldots, n_\sigma\}$ and $\tau_0 = \left(\sqrt{2n_s}\right)^{-1}$, $\tau = \left(\sqrt{2\sqrt{n_s}}\right)^{-i}$.

Mutation operator $\mathrm{mu}_\alpha : R^{n_\alpha} \to R^{n_\alpha}$ mutates the recombined values of the vector of inclination angles α:

$$\mathrm{mu}_\alpha(\alpha) := (\alpha_1 + z_1, \ldots, \alpha_1 + z_{n_\alpha}), \tag{22}$$

where $z_i \approx N(0, \beta^2)$ $\forall i \in \{1, 2, \ldots, n_\alpha\}$ with $\beta \cong 0.0873$ ($\cong 5°$).

Mutation operator $\mathrm{mu}_s : R^n \to R^n$ mutates the recombined values of the vector of continues design variables s, using the already mutated values of the σ and a

$$\mathrm{mu}_s(s) := (s_1 + \mathrm{cor}_1(\sigma, \alpha), \ldots, s_{n_s} + \mathrm{cor}_{n_s}(\sigma, \alpha)), \tag{23}$$

where cor is a random vector with normally distributed correlated components. The vector cor can be calculated according to $\mathrm{cor} = T \cdot z$ where $z = [z_1, \ldots, z_{n_\sigma}]^{\mathrm{T}}$ with $z_i \approx N(0, \sigma_i^2)\ \forall i \in \{1, \ldots, n_\sigma\}$ and

$$T = \prod_{p=1}^{n_\sigma - 1} \prod_{q=p+1}^{n_\sigma} T_{pq}(\tilde{a}_j), \tag{24}$$

where $j = 1/2(2n_\sigma - p)(p+1) - 2n_\sigma + q$ (Rudolph, 2001). The rotation matrices $T_{pq}(a_j)$ are unit matrices expect of the diagonal terms where $t_{pp} = t_{qq} = \cos(a_j)$ and $t_{pq} = -t_{qp} = -\sin(a_j)$.

7.3. Selection

There are two different types of selection schemes:

$(\mu + \lambda)$-ES: Where the best μ individuals are selected from a temporary population of $(\mu + \lambda)$ individuals to form the parents of the next generation.
(μ, λ)-ES: Where the μ individuals produce λ offsprings ($\mu \leqslant \lambda$) and the selection process defines a new population of μ individuals from the set of λ offsprings only.

Combining the recombination, mutation and selection operators the main loop for the case of (μ, λ)-ES is formulated as follows:

$$\mathrm{opt}_{(\mu+\lambda)\text{-ES}}(P^{(\mathrm{g})}) = \mathrm{sel}_\mu^\lambda \left(\bigcup_{i=1}^{\lambda} \left\{ \mathrm{mut}(\mathrm{rec}(P^{(\mathrm{g})})) \right\} \right). \tag{25}$$

While for the case of the $(\mu + \lambda)$-EA scheme the main loop is formulated as follows:

$$\mathrm{opt}_{(\mu+\lambda)\text{-ES}}(P^{(\mathrm{g})}) = \mathrm{sel}_\mu^{\mu+\lambda} \left(\bigcup_{i=1}^{\lambda} \left\{ \mathrm{mut}(\mathrm{rec}(P^{(\mathrm{g})})) \right\} \cup P^{(\mathrm{g})} \right). \tag{26}$$

The optimization procedure terminates when the following termination criterion is satisfied: the ratio μ_b/μ has reached a given value ε_d ($=0.8$ in the current study) where μ_b is the number of the parent vectors in the current generation with the best objective function value.

7.4. The ES algorithm

In Fig. 2 a pseudo-code of the ES algorithm is depicted. At the beginning of the procedure in generation $t = 0$ the initial parent population $P_{\mathrm{p}}^{(t)}$, composed by μ design vectors, is generated randomly (Step 3 of the pseudo-code). Steps 5–12 correspond to the main part of the ES algorithm, where in every generation λ offspring vectors are generated by means of recombination and mutation. D_l is a sub-population with two members selected from the parent population of the current generation $P_{\mathrm{p}}^{(t)}$ (Step 6) which is used by the recombination operator. Recombination and mutation operators, described in Steps 7–10, act on the both design variable vectors s_l and distribution parameter vectors σ_l and α_l (both distribution parameter vectors denoted as y_l in the pseudo-code). In Step 11, the objective and constraint functions are calculated in order to assess the design vectors in terms of the objective function value and feasibility.

7.5. ES for structural optimization problems

Structural optimization problems have been treated traditionally with mathematical programming algorithms, such as the sequential quadratic programming (SQP) method, which need gradient information. In

1. **Begin**
2. $t := 0$
3. $\text{initialize}\left(P_p^{(0)} := \left\{\left(y_m^{(0)}, s_m^{(0)}, F\left(s_m^{(0)}\right)\right),\ m = 1,\ldots,\mu\right\}\right)$
4. **Repeat**
5. **For** $l := 1$ **To** λ **Do Begin**
6. $D_l := \text{marriage}\left(P_p^{(t)}\right)$
7. $s_l := \text{s\_recombination}\left(D_l\right)$
8. $y_l := \text{y\_recombination}\left(D_l\right)$
9. $\tilde{s}_l := \text{s\_mutation}\left(s_l\right)$
10. $\tilde{y}_l := \text{y\_mutation}\left(y_l\right)$
11. $\tilde{F}_l := F\left(\tilde{s}_l\right)$
12. **End**
13. $P_o^{(t)} := \left\{\left(y_l^{(t)}, s_l^{(t)}, F\left(s_l^{(t)}\right)\right),\ l = 1,\ldots,\lambda\right\}$
14. **Case** selection_type **Of**
15. $(\mu,\lambda):\ P_p^{(t+1)} := \text{selection}\left(P_o^{(t)}, \mu\right)$
16. $(\mu+\lambda):\ P_p^{(t+1)} := \text{selection}\left(P_o^{(t)}, P_p^{(t)}, \mu\right)$
17. **End**
18. $t := t + 1$
19. **Until** termination_criterion
20. **End**

Fig. 2. Pseudo-code of the ES algorithm.

structural optimization problems, where the objective function and the constraints are particularly highly nonlinear functions of the design variables, the computational effort spent in gradient calculations is usually large. On the other hand EA optimization methods require more optimization steps.

In a number of studies by Papadrakakis et al. (1998, 1999) and Lagaros et al. (2002) it was found that EA optimization methods in structural optimization are computationally efficient even if large number of optimization steps is required to reach the optimum. These optimization steps are computationally less expensive than in the case of mathematical programming algorithms since they do not need gradient information. This property of probabilistic search methods is of greater importance in the case of RBO problems since the calculation of the derivatives of the reliability constraints is very time-consuming. Furthermore, probabilistic methodologies are considered, due to their random search, as global optimization methods because they are capable of finding the global optimum, whereas mathematical programming algorithms may be trapped in local optima.

8. Numerical examples

The hinged isotropic cylindrical panel of Fig. 3 is considered in order to illustrate the efficiency of the proposed reliability-based sizing-shape optimization methodology. The loading as well as the geometric and material properties of the perfect shell is also shown in Fig. 3. The curve edge nodes of the panel are assumed to be free in all directions while the nodes along the sides are hinged (fixed against translation). The material is considered to be elastic–perfectly plastic. The geometrically nonlinear elastic as well as elastoplastic response of point A of the perfect cylinder with respect to the applied vertical load P, is shown in Fig. 4, where the cylindrical panel is discretized with a 21×21 mesh of 400 TRIG shell elements. A mesh convergence study for this particular example is presented in a previous investigation (Argyris et al., 1998) where the computational

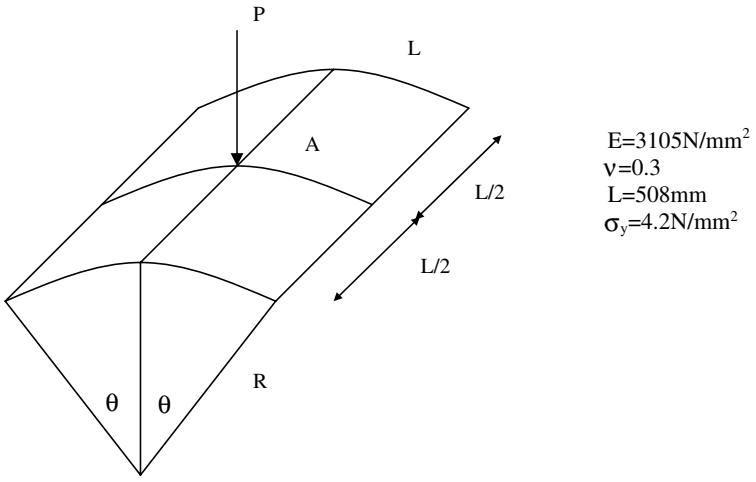

Fig. 3. Geometry, and material data of the cylindrical panel.

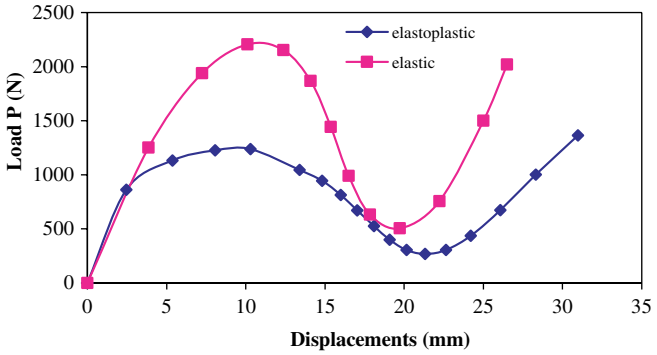

Fig. 4. Central load–displacement curve of the perfect cylindrical panel.

efficiency of the TRIC element in nonlinear shell analysis was demonstrated. For the discretization of the stochastic fields, the same mesh used for the finite element analysis is implemented since it is a fraction of the correlation length parameters adopted in this example. Thus, it is considered dense enough for the accurate representation of the fluctuations of the stochastic fields (Li and Der Kiureghian, 1992). The ultimate load of the perfect configuration is found to be $P_u = 2205$ N for the elastic shell and $P_u = 1240$ N for the elastoplastic.

8.1. Parametric investigation

A preliminary parametric investigation is presented with respect to the types and properties of the stochastic fields modeling the initial imperfections in order to conclude at realistic imperfections' scenarios that will be adopted subsequently in the optimization procedure. Both 1D and 2D stochastic imperfections are considered in order to investigate their effect on the buckling load of the panel. The thickness of the shell is considered to be equal to the height h at the apex, i.e., $t = 12.7$ mm. For all cases, the standard deviation σ_f of the stochastic field of the initial geometric imperfections is assumed to be $\sigma_f = 0.02h$, where h is the height at the apex of the cylindrical panel. For the stochastic fields describing the random material and thickness imperfections, the standard deviation was assumed $\sigma_f = 0.2$. Since no experimental data of initial imperfections is available for this specific type of structure, a parametric study was performed in previous investigations by Papadopoulos and Papadrakakis (2004, 2005), with respect to the correlation lengths of the stochastic fields in both x

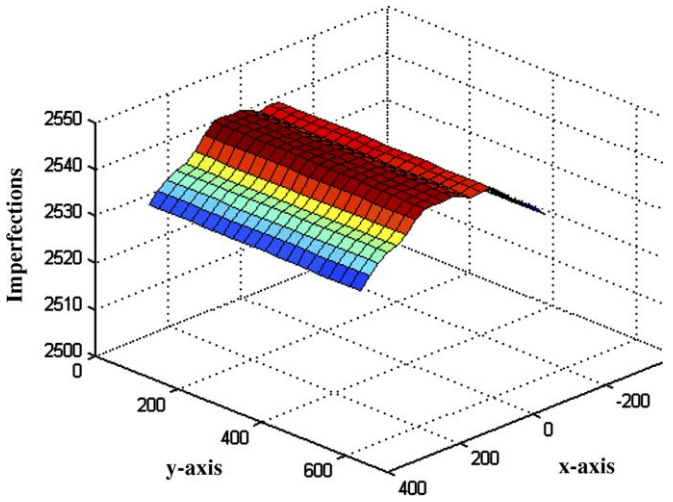

Fig. 5. One sample function of 1D random initial geometric imperfections for $\sigma_f = 0.10$ and $b_1 = 50$ mm.

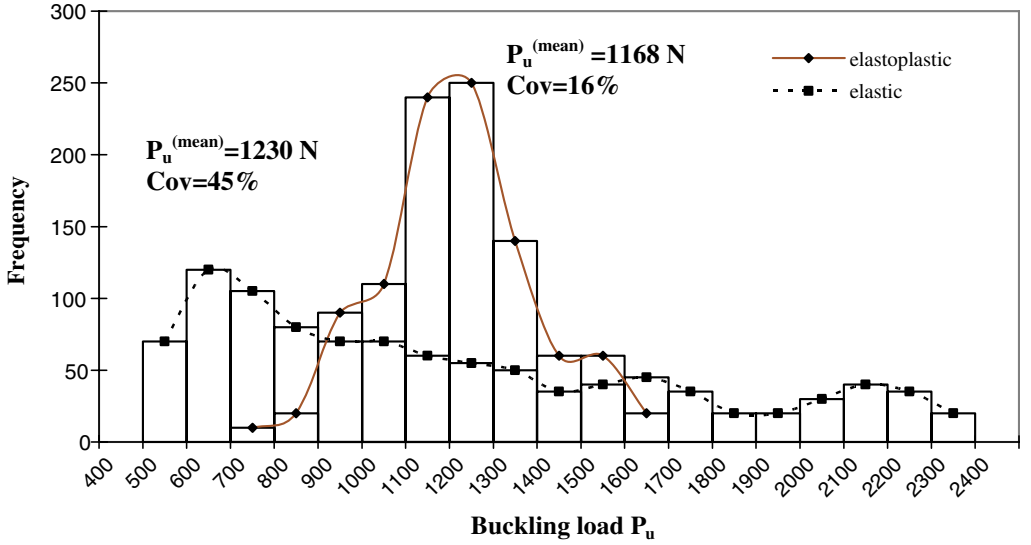

Fig. 6. Histograms of the critical load factor P_u for 1D variation of combined geometrical, material and thickness imperfections ($\sigma_f = 20\%$).

and y directions. The outcome of the parametric study was the evaluation of the "worst" imperfection mode of the shell, which led to the estimation of the lower bound of the buckling load of the shell. This information is most valuable for the safe design of shells against buckling.

As described in Li and Der Kiureghian (1992), for the 1D stochastic imperfections the "worst" imperfection pattern corresponds to a correlation length parameter $b_1 = 50$ mm for all random imperfection parameters (geometric, material and thickness). In that work, a Monte Carlo simulation procedure was performed in order to obtain the variability of the critical load factor of the panel for this correlation length parameter using a sample $N_{SAMP} = 100$. Fig. 5 presents one sample function of the initial geometric imperfections generated for the above mentioned correlation length parameter b_1 while Fig. 6 presents the histograms of the buckling loads for the same value of the parameter b_1, with and without physical nonlinearities. In the case where both geometric and physical nonlinearities are included, the mean value of the buckling load and the coefficient of variation are found to be 1168 N and 16%, respectively, while the lowest buckling load is computed at 700 N.

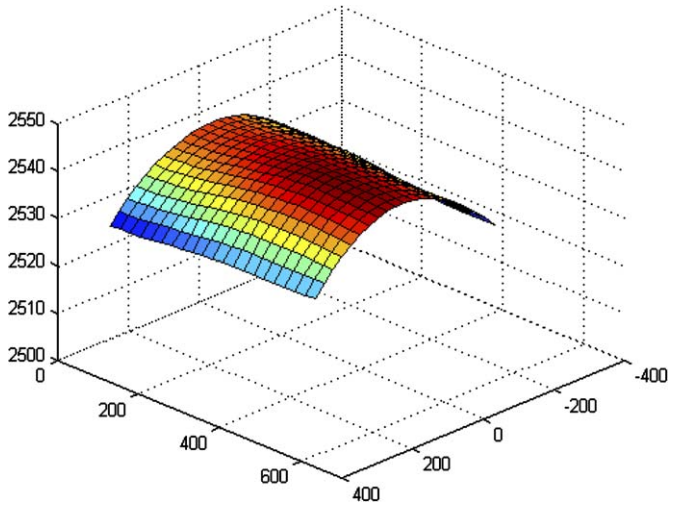

Fig. 7. One sample function of 2D random initial geometric imperfections for $\sigma_f = 0.20$ and $b_1 = b_2 = 250$ mm.

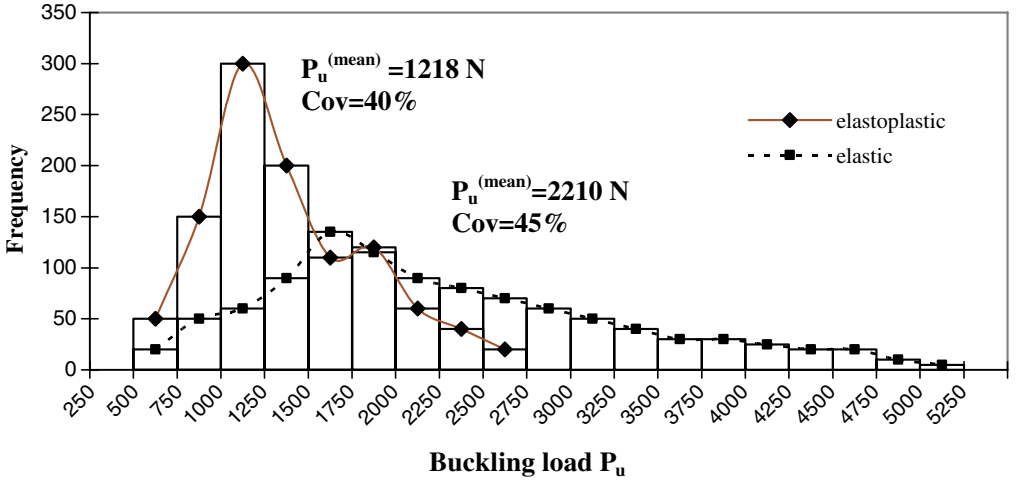

Fig. 8. Histograms of the critical load factor P_u for 2D variation of combined geometrical, material and thickness imperfections ($\sigma_f = 20\%$).

In the case in which only geometric nonlinearities are included, the mean value of the buckling load and the coefficient of variation was found to be 1230 N and 45%, respectively (Papadopoulos and Papadrakakis, 2004). The lowest buckling load for this case was computed at 500 N. It can be seen from Fig. 6 that a reduction of less than half of the coefficient of variation is computed in the elastoplastic model compared to the elastic one for the combined imperfections case, while the mean value of the buckling loads remains almost the same.

In the case of the 2D stochastic imperfections it is assumed that the correlation lengths in both x and y directions are equal, $b_1 = b_2$, since there are no specific manufacturing procedures or boundary conditions that would indicate a different assumption. The "worst" imperfection mode for this case corresponds to a correlation length parameter $b_1 = b_2 = 250$ mm for the initial geometric imperfections, while the corresponding to the random material and thickness imperfections values were found to be $b_1 = b_2 = 50$ mm (Papadopoulos and Papadrakakis, 2004, 2005). In Fig. 7 one sample function of initial geometric imperfections generated for the aforementioned correlation parameter is presented, while Fig. 8 presents the histograms of the buckling loads for this "worst" imperfections' pattern, with and without physical nonlinearities. In the case where both

geometric and physical nonlinearities are included, the mean value of the buckling load is found to be 1218 N with a coefficient of variation (cov) 40%. The lowest buckling load is estimated at 500 N for this case. In the case in which only geometric nonlinearities are included, the mean value of the buckling load was found to be 2170 N and the coefficient of variation (cov) 45% (Papadopoulos and Papadrakakis, 2004). In this case the lowest buckling load was also estimated at 500 N. For this case, a reduction of about 50% of the mean value of the buckling loads is computed in the elastoplastic panel with respect to the elastic one, while the coefficient of variation remains the almost the same.

8.2. Optimization results

Following the results of the preliminary previously described preliminary investigation, RBDO is performed for the above mentioned imperfections' scenario. Two design variables of the shell structure are considered and the weight of the structure is the objective to be minimized. In the formulation of the RBDO problem, the probabilistic constraint is imposed on the probability of structural failure and is set to $p_a = 0.001$. For each set of design parameters generated by the evolutionary algorithm, the probability of failure caused by uncertainties related to material properties, geometry and loads of the structures is estimated using a brute-force MCS with $N_{\mathrm{SAMP}} = 1000$. For this calculation, the concentrated load acting at point A of the shell (see Fig. 3) is described as a random variable assumed to follow a log–normal probability density function with mean value equal to 1000 N and standard deviation equal to 100 N.

Two kinds of design variables are examined for the test example considered, shape and sizing ones. The shape design variable refers to the selection of the optimum curvature of the shell, which is defined by the angle θ, while the sizing design variable refers to the selection of the shell thickness. A deterministic (DBO) and a probabilistic (RBDO) based formulations of the optimum design of a shell structure are considered in this study. The DBO formulation is implemented considering linear and elastoplastic behavior. The DBO formulation with elastic behavior can be stated as follows:

$$\begin{aligned} &\min && \mathrm{weight}(\theta, t) \\ &\text{subject to} && \left.\begin{array}{l} 0^\circ \leqslant \theta \leqslant 10^\circ \\ 5\ \mathrm{mm} \leqslant t \leqslant 25\ \mathrm{mm} \end{array}\right\} \text{bounds of the design variables} \\ & && \sigma_{\text{von Mises}} \leqslant \sigma_{\mathrm{y}}/1.10, \quad \sigma_{\mathrm{y}} = 4.2\ \mathrm{N/mm^2}. \end{aligned} \tag{27}$$

The DBO formulation with elastoplastic behavior can be stated as follows

$$\begin{aligned} &\min && \mathrm{weight}(\theta, t) \\ &\text{subject to} && \left.\begin{array}{l} 0^\circ \leqslant \theta \leqslant 10^\circ \\ 5\ \mathrm{mm} \leqslant t \leqslant 25\ \mathrm{mm} \end{array}\right\} \text{bounds of the design variables} \\ & && P_{\mathrm{buckl}} \geqslant 1000\ \mathrm{N}. \end{aligned} \tag{28}$$

The difference between the two DBO formulations is the constraints imposed either on the maximum von Mises stress or on the buckling load in the case of the elastoplastic behavior. Four distinctive formulations of the RBDO problem are examined, considering either elastic or elastoplastic behavior while 1D and 2D combined random imperfections are taken into account. The RBDO formulations with elastic behavior can be defined as

$$\begin{aligned} &\min && \mathrm{weight}(\theta, t) \\ &\text{subject to} && \left.\begin{array}{l} 0^\circ \leqslant \theta \leqslant 10^\circ \\ 5\ \mathrm{mm} \leqslant t \leqslant 25\ \mathrm{mm} \end{array}\right\} \text{bounds of the design variables} \\ & && \sigma_{\text{von Mises}} \leqslant \sigma_{\mathrm{y}}/1.10 \text{ deterministic constraint}, \\ & && p_f \leqslant 0.1\% \text{ probabilistic constraint}, \end{aligned} \tag{29}$$

with 1D and 2D combined random imperfections, while the RBDO formulation with elastoplastic behavior can be stated as follows:

Table 1
Formulation of the optimization problem – a comparative study

Optimization problem formulation	Design (angle θ, thickness t)	Volume (cm^3)	Generations	Time (h)	p_f[a] (%)
DBO linear	2.3°, 9.3 mm	4801	24	0.07	8.3
DBO elastoplastic	2.8°, 10.2 mm	5267	23	0.50	3.9
RBDO elastic 1D imperfection	6°, 12 mm	6205	15	210.0	0.3
RBDO elastoplastic 1D imperfection	4.9°, 14.5 mm	7493	19	261.7	0.1
RBDO elastic 2D imperfection	5.3°, 11.2 mm	5789	14	183.4	0.5
RBDO elastoplastic 2D imperfection	5.1°, 14.5 mm	7494	16	216.8	0.1

[a] Calculated considering elastoplastic behavior with 2D imperfections.

$$\begin{aligned} &\min && \text{weight}(\theta, t) \\ &\text{subject to} && \left.\begin{aligned} &0^\circ \leqslant \theta \leqslant 10^\circ \\ &5\ \text{mm} \leqslant t \leqslant 25\ \text{mm} \end{aligned}\right\} \text{bounds of the design variables,} \\ & && p_f \leqslant 0.1\% \text{ probabilistic constraint,} \end{aligned} \tag{30}$$

considering 1D and 2D combined random imperfections. In all formulations of the optimization problem the ES algorithm was employed, while the number of parent and offspring vectors is taken equal to 5 (i.e., the $(5+5)$-ES optimization scheme is adopted). Table 1 presents the results of the optimization procedure for all DBO and RBDO formulations considered.

As it can be observed from Table 1, the optimum weight achieved based on the DBO formulation considering elastoplastic behavior is 10% more than the deterministic one with linear behavior. On the other hand, in the case of the RBDO formulation of the optimization problem, the optimum weight achieved considering elastoplastic behavior is increased by 21% and 30% for 1D and 2D imperfections; respectively, compared to the elastic behavior. The detailed formulation of the optimization problem considering elastoplastic behavior and 2D imperfections is by 56% and 42% heavier that the optimum design achieved with the DBO formulation considering elastic and elastoplastic behavior, respectively.

In Table 1 can also be seen the computing time required for the three different formulations of the optimization problem. The RDBO formulation is orders of magnitude more time consuming that the DBO formulations. The importance, though, of considering an RBDO formulation instead of a DBO one can be seen from the probability of failure that corresponds to the optimum designs achieved with the three different formulations. All probabilities of failure reported in Table 1 have been computed considering elastoplastic behavior and 2D imperfections for all six optimum design cases examined. As can be seen the probability of failure corresponding to the optimum computed by the deterministic optimization procedure, with linear formulation or with elastoplastic behavior, is one order of magnitude larger than the allowable limit value, equal to 10^{-3}, considered in this work. On the other hand there is difference, both in terms of optimum weight and probability of failure, between the optimum designs achieved when considering the RDBO formulation with either elastic or elastoplastic behavior.

9. Conclusions

In most cases optimum design of structures is based on deterministic parameters and is focused on the satisfaction of the associated deterministic constraints. So far, many articles have been devoted to this research field and efficient methods have been presented. Since there are many random factors that affect the behavior, the manufacturing and the life of a structure the deterministic optimum is not indeed the "real" optimum. In order to find the "real" optimum the designer has to take into account all necessary random parameters and via the reliability analysis of the structure to determine its optimum design taking into account a given probability of failure. Only after forming and solving this RBDO problem, even with additional cost in weight and computing time, a "global" optimum structural design can be found.

Along these lines, an efficient RBDO procedure is proposed for the sizing-shape optimization of shell-type structures with random initial geometric material and thickness imperfections. In particular, the effect of

material and thickness imperfections on the buckling load of isotropic shells is investigated with respect to the optimum design of a cylindrical panel. For this purpose, the concept of an initial "imperfect" structure is introduced involving not only geometric deviations of the shell structure from its perfect geometry but also a spatial variability of the modulus of elasticity as well as of the thickness of the shell. For the RDBO formulation, the objective function is assumed to be the weight of the structure while the constraints are taken both deterministic (stress and displacement limitations) and probabilistic (the overall probability failure of the structure). It is assumed that structural failure occurs when buckling load of the shell is reached. Then, the overall probability of failure is taken as the global probabilistic constraint. Numerical results are presented for a cylindrical panel, demonstrating the efficiency as well as the applicability of the proposed methodology in obtaining rational optimum designs of shell-type structures in the presence of random geometric, material and thickness imperfections.

References

Allen, M., Maute, K., 2005. Reliability-based shape optimization of structures undergoing fluid–structure interaction phenomena. Comput. Meth. Appl. Mech. Eng. 194 (30–33), 3472–3495.

Arbocz, J., 2001. The effect of imperfect boundary conditions on the collapse behaviour of anisotropic shells. Int. J. Solids Struct. 37, 6891–6915.

Arbocz, J., Abramovich, H., 1979. The initial imperfection data bank at the Delft University of Technology, Part 1. Technical Report LR-290, Delft University of Technology, Department of Aerospace Engineering.

Arbocz, J., Hol, J.M.A.M., 1991. Collapse of axially compressed cylindrical shells with random imperfections. AIAA J. 29 (12), 2247–2256.

Argyris, J.H., Tenek, L., Olofsson, L., 1997. TRIC, A simple but sophisticated 3 node triangular element based on 6 rigid-body and 12 straining modes for fast computational simulations of arbitrary isotropic and laminated composite shells. Comput. Meth. Appl. Mech. Eng. 145, 11–85.

Argyris, J.H., Tenek, L., Papadrakakis, M., Apostolopoulou, C., 1998. Postbuckling performance of the TRIG natural mode triangular element for isotropic and laminated composite shells. Comput. Meth. Appl. Mech. Eng. 166, 211–231.

Argyris, J.H., Papadrakakis, M., Karapitta, L., 2002a. Elastoplastic analysis of shells with the triangular element TRIC. Comput. Meth. Appl. Mech. Eng. 191 (33), 3613–3637.

Argyris, J.H., Papadrakakis, M., Stefanou, G., 2002b. Stochastic finite element analysis of shells. Comput. Meth. Appl. Mech. Eng. 191 (41–42), 4781–4804.

Deml, M., Wunderlich, W., 1997. Direct evaluation of the 'worst' imperfection shape in shell buckling. Comput. Meth. Appl. Mech. Eng. 149, 201–222.

Elishakoff, I., 2000. Uncertain buckling: its past, present and future. Int. J. Solids Struct. 37, 6869–6889.

Elishakoff, I., Arbocz, J., 1982. Reliability of axially compressed cylindrical shells with random axisymmetric imperfections. Int. J. Solids Struct. 18, 563–585.

Elishakoff, I., Arbocz, J., 1985. Reliability of axially compressed cylindrical shells with general nonsymmetric imperfections. J. Appl. Mech. 52, 22–128.

Elishakoff, I., Van Manen, S., Vermeulen, P.G., Arbocz, J., 1987. First-order second-moment analysis of the buckling of shells with random imperfections. AIAA J. 25 (8), 1113–1117.

Eurocode 3, 1993. Design of steel structures, Part 1.1: General rules; Part 1.5: Strength and stability of planar plated structures without transverse loading. European Committee for Standardization, January 1993.

Hurtado, J.E., Barbat, A.H., 1997. Simulation methods in stochastic mechanics. In: Marczyk, J. (Ed.), Computational Stochastic Mechanics in a Meta-computing Perspective. CIMNE, Barcelona, pp. 93–116.

Lagaros, N.D., Papadrakakis, M., Kokossalakis, G., 2002. Structural optimization using evolutionary algorithms. Comp. Struct. 80 (7–8), 571–587.

Lagaros, N.D, Plevris, V., Papadrakakis, M., 2005. Multi-objective design optimization using cascade evolutionary computations. Comput. Meth. Appl. Mech. Eng. 194 (30–33), 3496–3515.

Lee, K.-H., Park, G.-J., 2001. Robust optimization considering tolerances of design variables. Comp. Struct. 79, 77–86.

Li, C.-C., Der Kiureghian, A., 1992. An optimal discretization of random fields. Technical Report UCB/SEMM-92/04, Department of Civil Engineering, University of Berkeley, California, USA.

Li, Y.W., Elishakoff, I., Starnes Jr., J.H., Bushnell, D., 1997. Effect of the thickness variation and initial imperfection on buckling of composite shells: asymptotic analysis and numerical results by BOSOR4 and PANDA2. Int. J. Solids Struct. 34, 3755–3767.

Messac, A., Ismail-Yahaya, A., 2002. Multiobjective robust design using physical programming. Struct. Multidisc. Optim. 23, 357–371.

Noh, H.-C., 2006. Effect of multiple uncertain material properties on the response variability of in-plane and plate structures. Comput. Meth. Appl. Mech. Eng. 195 (19–22), 2697–2718.

Noh, H.-C., Kwak, H.-G., 2006. Response variability due to randomness in Poisson's ratio for plane-strain and plane-stress states. Int. J. Solids Struct. 43 (5), 1093–1116.

Palassopoulos, G.V., 1997. Buckling analysis and design of imperfection sensitive structures. In: Haldar, A., Guran, A., Ayyub, B.M. (Eds.), Uncertainty Modeling in Finite Element, Fatigue and Stability of Systems, Series on Stability, Vibration and Control of System Series B, vol. 9. World Scientific publishing Company, Singapore, pp. 311–356.

Papadopoulos, V., Papadrakakis, M., 2004. Finite element analysis of cylindrical panels with random initial imperfections. J. Eng. Mech., ASCE 130 (8), 867–876.

Papadopoulos, V., Papadrakakis, M., 2005. The effect of material and thickness imperfections on the buckling load of shells with random initial imperfections. Comput. Meth. Appl. Mech. Eng. 194 (12–16), 1405–1426.

Papadrakakis, M., Lagaros, N.D., 2002. Reliability-based structural optimization using neural networks and Monte Carlo simulation. Comput. Meth. Appl. Mech. Eng. 191 (32), 3491–3507.

Papadrakakis, M., Lagaros, N.D., Thierauf, G., Cai, J., 1998. Advanced solution methods in structural optimization based on evolution strategies. J. Eng. Comput. 15 (1), 12–34.

Papadrakakis, M., Tsompanakis, Y., Lagaros, N.D., 1999. Structural shape optimization using evolution strategies. Eng. Optim. 31, 515–540.

Qu, X., Haftka, R.T., Venkataraman, S., 2003. Deterministic and reliability-based optimization of composite laminates for cryogenic environments. AIAA J. 41 (10), 2029–2036.

Rudolph, G., 2001. Self-adaptive mutations may lead to premature convergence. IEEE Trans. Evolut. Comput. 5 (4), 410–414.

Schenk, C.A., Schueller, G.I., 2003. Buckling analysis of cylindrical shells with random geometric imperfections. Int. J. Non-Linear Mech. 38, 1119–1132.

Schueller, G.I., 2001. Computational stochastic mechanics – recent advances. Comp. Struct. 79 (22–25), 2225–2234.

Schwefel, H.P., 1981. Numerical Optimization for Computer Models. Wiley & Sons, Chichester, UK.

Shinozuka, M., Deodatis, G., 1996. Simulation of multi-dimensional Gaussian stochastic fields by spectral representation. Appl. Mech. Rev., ASME 49, 29–53.

Stefanou, G., Papadrakakis, M., 2004. Stochastic finite element analysis of shells with combined random material and geometric properties. Comput. Meth. Appl. Mech. Eng. 193 (1–2), 139–160.